Synthesis of PNIPAM Polymer Brushes on Reduced Graphene Oxide Based on Click Chemistry and RAFT Polymerization

Yongfang Yang,[1] Xiaohui Song,[2] Liang Yuan,[2] Mao Li,[1] Jinchuan Liu,[2] Rongqin Ji,[1] Hanying Zhao[2]

[1]Institute of Polymer Science and Engineering, Hebei University of Technology, Tianjin 300130, People's Republic of China
[2]Key Laboratory of Functional Polymer Materials, Ministry of Education, Department of Chemistry, Nankai University, Tianjin 300071, People's Republic of China
Correspondence to: H. Zhao (E-mail: hyzhao@nankai.edu.cn)

Received 9 August 2011; accepted 4 October 2011; published online 22 October 2011
DOI: 10.1002/pola.25036

ABSTRACT: Preparation and characterization of poly(*N*-isopropylacrylamide) (PNIPAM) polymer brushes on the surfaces of reduced graphene oxide (RGO) sheets based on click chemistry and reversible addition-fragmentation chain transfer (RAFT) polymerization was reported. RGO sheets prepared by thermal reduction were modified by diazonium salt of propargyl *p*-aminobenzoate, and alkyne-functionalized RGO sheets were obtained. RAFT chain transfer agent (CTA) was grafted to the surfaces of RGO sheets by click reaction. PNIPAM on RGO sheets was prepared by RAFT polymerization. Fourier transform-infrared spectroscopy, thermogravimetric analysis, X-ray photoelectron spectroscopy, and transmission electron microscopy (TEM) results all demonstrated that RAFT CTA and PNIPAM were successfully produced on the surfaces of RGO sheets. Nanosized PNIPAM domains on RGO sheets were observed on TEM. Micro-DSC result indicated that in aqueous solution PNIPAM on RGO sheets presented a lower critical solution temperature at 33.2 °C. © 2011 Wiley Periodicals, Inc. J Polym Sci Part A: Polym Chem 50: 329–337, 2012

KEYWORDS: click chemistry; living radical polymerization (LRP); nanocomposites; poly(*N*-isopropylacrylamide) (PNIPAM); polymer brushes; reduced graphene oxide; reversible addition-fragmentation chain transfer (RAFT) polymerization

INTRODUCTION Graphene, a single-atom-thick sheet of sp2-bonded carbon atoms, is the basal building block of all graphitic materials.[1] Since its discovery in 2004, graphene-based materials have attracted considerable attention because of their excellent mechanical, optical, and electrical properties.[2–4] Graphene-based polymer materials also triggered enormous interest for extremely high thermal conductivity and strong mechanical properties.[5]

Graphene sheets tend to agglomerate through van der Waals interaction due to their high specific surface area. In order to increase the dispersibility of the graphene sheets in organic solvents or in polymer matrix, graphene sheets are functionalized by covalent modification or noncovalent coupling modifications.[6–8] Because of the inherent instability of the resulting supramolecular systems, it is difficult to control the structure of graphene modified by noncovalent method,[9] and the chemical modification of graphene is of great importance in the preparation of graphene composites with stable structures.[10,11]

There are two approaches to the covalent modification of the graphene sheets. The first one is related to the chemical reactions of hydrophilic functional groups on the graphene sheets, such as —OH and —COOH groups.[12,13] The second approach is to take advantage of addition chemistry in graphene modification, such as nitrene addition,[14] diazonium coupling,[15] and 1,3-dipolar cycloaddition.[16] In these years, click chemistry, especially Cu(I)-catalyzed 1,3-dipolar azide-alkyne cycloaddition reaction, has gained a great deal of attention due to excellent functional group tolerance, high specificity, and nearly quantitative yields under mild experimental conditions.[17] A variety of functional polymers and materials with different structures were prepared based on click chemistry. For example, Sun et al. used click chemistry to functionalize graphene sheets.[18] They synthesized azido-terminated polystyrene (PS) by atom transfer radical polymerization (ATRP) using 3-azidoethyl 2-bromoisobutyrate as initiator. Graphite oxide sheets were functionalized by propargyl alcohol through an acylation reaction, and the click reaction between alkyne functionalized sheets and azido-terminated PS was conducted at room temperature. He and Gao reported a unified approach to covalently functionalize graphene nanosheets based on nitrene chemistry.[19] Many different functional moieties (hydroxyl, carboxyl, amino, bromine,

Additional Supporting Information may be found in the online version of this article.

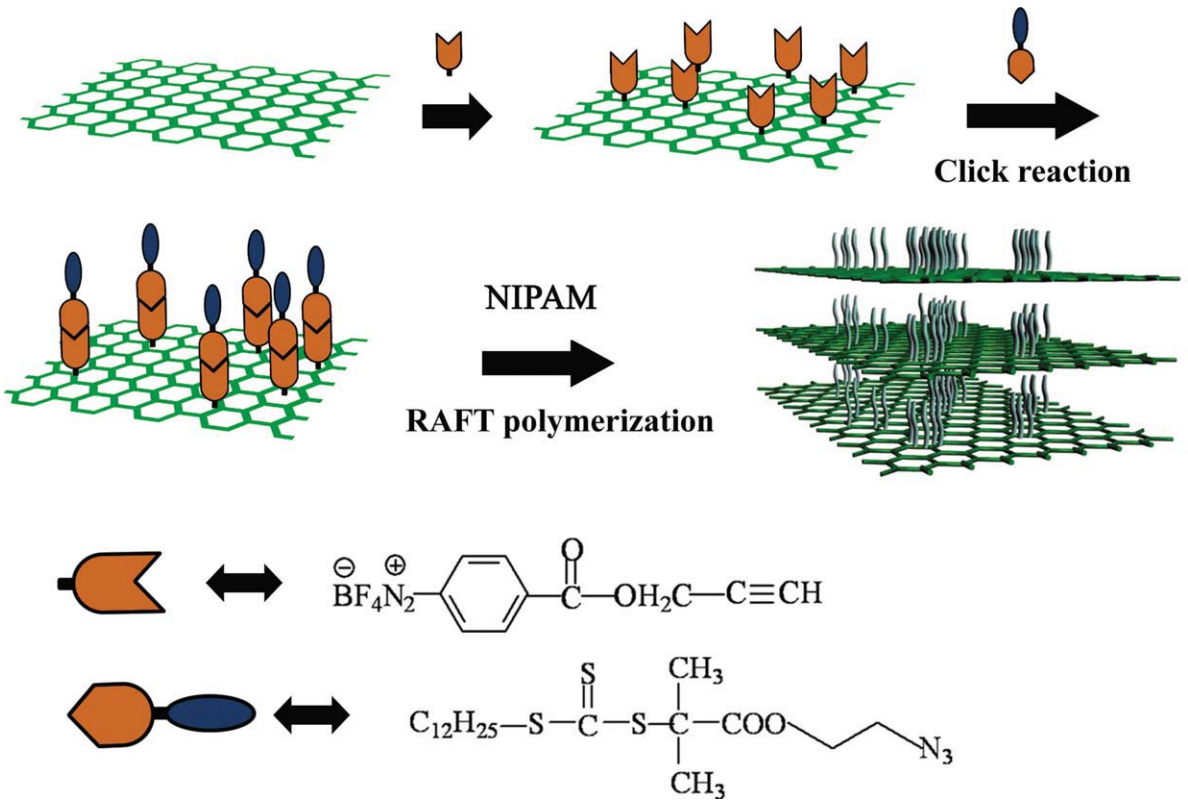

SCHEME 1 Outline for the preparation of PNIPAM/reduced graphene oxide (RGO) nanocomposites based on click chemistry and RAFT polymerization.

long alkyl chain, etc.) and polymers (e.g., poly(ethylene glycol), polystyrene) were anchored to the graphene sheets by this approach. Although this strategy is simple and efficient, the reaction is time consuming and the reaction temperature is high.

Combination of click chemistry and reversible addition-fragmentation chain transfer (RAFT) polymerization provides an efficient method for the synthesis of new polymers and materials.[20–22] We synthesized new comb polymers and nanohydrogels based on this method.[23–25] *In situ* polymerization on the surfaces of reduced graphene oxide (RGO) sheets provides a versatile method for the fabrication of RGO/polymer nanocomposites. In a previous article, we reported an efficient process for modification of RGO sheets. ATRP initiator was grafted onto the RGO sheets by reaction of 2-bromo-2-methylpropionyl bromide with amine groups and hydroxyl groups on the RGO sheets, and poly(2-(dimethylamino)ethyl methacrylate) were prepared on the surfaces of RGO sheets by *in situ* ATRP.[26] In this article, for the first time we report the functionalization of RGO based on click chemistry and RAFT polymerization. RGO sheets were treated by thermal reduction. Alkyne groups were introduced onto the RGO sheets by a reaction of RGO sheets with aryldiazonium salts containing alkyne groups. Azido-terminated RAFT chain transfer agent (CTA) was synthesized by reaction of 3-azido-1-propanol and *S*-1-dodecyl-*S*′-(α,α′-dimethyl-α″-acetic acid) trithiocarbonate. RAFT CTA was grafted to the RGO sheets by facile click reaction, and *N*-isopropylacrylamide (NIPAM) was polymerized on RGO sheets via RAFT polymerization method (Scheme 1).

EXPERIMENTAL

Materials

Natural flake graphite with an average particle size of 40 μm (99%) was purchased from Qingdao Guangyao Graphite Co. Fuming nitric acid (>90%) was purchased from Tianjin FengChuan Chem. Co. Sulfuric acid (98%), potassium chlorate (98%), and hydrochloric acid (37%) were purchased from Tian Jin Institute of Chemical Agents and used as received. NIPAM (97%) was purchased from Aldrich. Before use, it was recrystallized from hexane and dried under vacuum. Copper (I) bromide (CuBr) was purchased from Guo Yao Chemical Company and was purified by washing with glacial acetic acid. *N*,*N*,*N*,*N*,*N*-Pentamethyldiethylenetriamine (PMDETA, 99%), sodium azide (Alfa, 99%), 2-bromo-2-methyl propionyl bromide (98%), and 3-bromo-1-propanol (98%) were purchased from Aldrich and used as received. 2,2′-Azobis(isobutyronitrile) (AIBN) was purchased from Guo Yao Chemical Co. and was purified by recrystallization from ethanol. *S*-1-Dodecyl-*S*′-(α,α′-dimethyl-α″-acetic acid) trithiocarbonate was synthesized according to the previous literature.[27] *N*-(3-(dimethylamino)propyl)-*N*′-ethylcarbodiimide hydrochloride (EDC.HCl) purchased from Shanghai Medpep Co., *p*-aminobenzoic acid purchased from Tianjin Guangfu chemical Company, 4-(dimethylamino) pyridine

(DMAP, Alfa), and nitrosyl tetrafluoroborate (Alfa) were used as received. All the solvents were distilled before use.

Preparation of RGO Sheets

Graphite oxide (GO) were prepared according to the Staudenmaier method.[28,29] Graphite (5 g) was reacted with concentrated nitric acid (45 mL) and sulfuric acid (87.5 mL) in the presence of potassium chlorate (55 g). On completion of the reaction, the mixture was added to excess water, and washed with HCl aqueous solution (5%) and water until the pH of the filtrate was neutral. The dried sample was stored in a vacuum oven at 60 °C before use. Thermal reduction of GO was conducted by placing the sample in a Muffle Furnace preheated to 950 °C and held in the furnace for 30 s.

Synthesis of Propargyl *p*-Aminobenzoate and its Diazonium Salt

EDC.HCl (5.26 g), DMAP (0.30 g), and *p*-aminobenzoic acid (3.14 g) were dissolved in 75 mL of $CHCl_3$, and 1.70 mL of propargyl alcohol was added dropwise into the mixture at 0 °C. The solution was stirred at 0 °C for 2 h and at room temperature for 2 days. The reaction mixture was washed with 20 mL of doubly distilled water and the organic layer was collected and dried over magnesium sulfate, and concentrated under reduced pressure. The product was purified by column chromatography (eluent: petroleum ether: ethyl acetate: dichloromethane = 5:1:1), and yellow liquid was collected. After removal of the solvent, solid product was obtained. The yield of the product is about 65%. ^{1}H NMR (400 MHz, $CDCl_3$, δ): 2.49(s,1H, —C≡*CH*), 4.10 (s, 2H, —*NH*$_2$), 4.89 (s, 2H, —O*CH*$_2$—), 6.66 and 7.90 (t, 4H, Ar *H*).

The synthesis of diazonium salt of propargyl *p*-aminobenzoate was described as follows.[6] Nitrosyl tetrafluoroborate (0.48 g) was dissolved in 10 mL of acetonitrile, and propargyl *p*-aminobenzoate (0.6 g) in 3.4 mL of acetonitrile solution was added at −30 °C. The solution was stirred at 0 °C for 0.5 h and at room temperature for 1 h. After the reaction, 30 mL of ether was added to the solution and solid product was obtained. The solids was washed by ether and dried in vacuum oven at room temperature.

Synthesis of Azido-Terminated Trithiocarbonate

S-1-dodecyl-*S*′-(α,α′-dimethyl-α″-acetic acid) trithiocarbonate and 3-azido-1-propanol were synthesized according to the previous literature.[27,30] *S*-1-dodecyl-*S*′-(α,α′-dimethyl-α″-3-azido-1-propyl acetate) trithiocarbonate was synthesized by esterification of *S*-1-dodecyl-*S*′-(α,α′-dimethyl-α″-acetic acid) trithiocarbonate and 3-azido-1-propanol. *S*-1-Dodecyl-*S*′-(α,α′-dimethyl-α″-acetic acid) trithiocarbonate (1.03 g, 2.75 mmol), 4-dimethylaminopyridine (35 mg, 0.27 mmol), and methylene dichloride (20 mL) were added into a round bottomed flask. The flask was immersed in an ice bath, and EDC.HCl (1.08 g, 5.49 mmol) was added. After stirring at 0 °C for 0.5 h, 3-azido-1-propanol (0.56 g, 5.5 mmol) in 6 mL of dry methylene dichloride was added dropwise. The solution was stirred at 0 °C for 2 h and at room temperature for 2 days. After the reaction, the solution was diluted with 20 mL of dichloromethane, and washed with saturated sodium bicarbonate aqueous solution. The organic layer was collected, dried over magnesium sulfate, and concentrated under reduced pressure. The product was purified by column chromatography (eluent: petroleum ether: ethyl acetate = 90:10) to obtain yellow liquid. The yield of the product is about 75%. ^{1}H NMR (400 MHz, $CDCl_3$, δ): 4.19 (s, 2H, —O—*CH*$_2$—$(CH_2)_2$—N_3), 3.36 (t, 2H, —C*H*$_2$—N_3), 3.28 (t, 2H, —S—*CH*$_2$—$(CH_2)_{10}$—CH_3), 1.91 (t, 2H, —*CH*$_2$—CH_2—N_3), 1.70 (s, 6H —CO—C(*CH*$_3$)$_2$—COO—), 1.27–1.68 (m, 20H, —*C*$_{10}$*H*$_{20}$—), 0.89 (t, 3H, —CH_2—*CH*$_3$).

Preparation of RAFT CTA-Modified RGO

At the first step of modification, RGO sheets were modified by diazonium salt of propargyl *p*-aminobenzoate,[6] and alkyne-functionalized RGO sheets were obtained. The details were described as follows: RGO (20 mg) was dispersed in 20 mL of doubly distilled water at pH 10, and diazonium salt was added into the solution (0.11 mmol/mL). The solution was stirred at room temperature overnight. The mixture was diluted with 100 mL of acetone. Modified RGO sheets were obtained after filtration and washing with water, DMF, and acetone. The resulting solid was dried in a vacuum oven at 50 °C.

RAFT CTA-modified RGO was prepared by click reaction between alkynes functionalized RGO sheets and RAFT agent. Alkyne-functionalized RGO (16 mg) was dispersed into 5 mL of DMF. After sonication, *S*-1-dodecyl-*S*′-(α,α′-dimethyl-α″-3-azido-1-propyl acetate) trithiocarbonate (60 mg, 0.015 mmol), PMDETA (3.0 μL, 0.015 mmol), and CuBr (2.2 mg, 0.015 mmol) were added into the solution. The solution was stirred at room temperature for 25 h under nitrogen atmosphere. The RAFT CTA-modified RGO was obtained by centrifugation. After washing with DMF and CH_3OH, the RGO sheets were dried in a vacuum oven at 40 °C for 2 days.

RAFT Polymerization of NIPAM on RGO Sheets

A typical polymerization was described as follows. RAFT CTA-modified RGO (8.8 mg, 0.0030 mmol RAFT CTA) was dispersed in 2 mL of DMF under ultrasonication. NIPAM monomer (113.2 mg, 1.000 mmol) and AIBN (0.164 mg, 0.0010 mmol) were added into the dispersion. RAFT polymerization was conducted at 60 °C for 20 h under nitrogen atmosphere. After polymerization, the nanocomposite was collected via centrifugation, and was dried in a vacuum oven at 40 °C for 2 days.

Characterization

^{1}H NMR (400 MHz) spectra were recorded on a Varian UNITY-plus 400 spectrometer. The thermal properties of the nanocomposites were measured by thermogravimetric analysis (TGA). The samples were heated to 800 °C at a heating rate of 10 K/min under nitrogen atmosphere on a Netzsch TG 209. High-resolution transmission electron microscope (TEM) observations were carried out on a Tecnai G220 S-TWIN electron microscope equipped with a Model 794 CCD camera (512 × 512). TEM specimens were prepared by dipping copper grids into solutions and drying in air. The TEM specimens with PNIPAM were stained by OsO_4. The apparent molecular weight and molecular weight distribution of PNIPAM were determined with a gel permeation chromatograph (GPC) equipped with a waters 717 autosampler, waters 1525 HPLC pump, three waters Ultra Styragel columns with 5K-600K (10,000 Å), 500-30K (1000 Å), and

100-10K (500 Å) molecular ranges, and a waters 2414 Refractive Index Detector. Atomic force microscopy (AFM) images were collected on a Nanoscope IV atomic force microscope (Digital Instruments). The microscope was operated in tapping mode using Si cantilevers with a resonance frequency of 320 KHz. The voltage was between 2 and 3 V, and a tip radius was less than 10 nm. A drive amplitude of 1.2 V, and a scan rate of 1.0 Hz were used. Fourier transform-infrared absorption spectra (FTIR) were obtained on a Bio-Rad FTS 6000 system using diffuse reflectance sampling accessories. The micro-DSC measurements were performed on a VP-DSC microcalorimeter (MicroCal). X-ray photoelectron spectroscopy (XPS) spectra were recorded on a Kratos Axis Ultra delay line detector (DLD) spectrometer employing a monochromated Al-Kα X-ray source ($h\nu$ = 1486.6 eV), hybrid (magnetic/electrostatic) optics, and a multichannel plate and DLD. All XPS spectra were recorded using an aperture slot of 300 to 700 microns, survey spectra were recorded with pass energy of 160 eV, and high-resolution spectra were recorded with pass energy of 40 eV.

RESULTS AND DISCUSSION

The synthesis of RAFT CTA-modified RGO and RAFT polymerization of NIPAM on RGO sheets were shown in Scheme 2. RGO sheets were modified by diazonium salt of propargyl *p*-aminobenzoate, and alkyne-functionalized RGO sheets were obtained. RAFT CTA was grafted to the surfaces of RGO sheets by click reaction. PNIPAM brushes on RGO sheets were prepared by RAFT polymerization. Propargyl *p*-aminobenzoate was synthesized by reaction of *p*-aminobenzoic acid and propargyl alcohol in the presence of EDC.HCl and DMAP. ^{1}H NMR spectrum of the compound was shown in Supporting Information Figure S1. The peaks at 2.5 and 4.9 ppm are attributed to the alkyne proton (—C≡C***H***), and the methene protons next to the ester group (—O—C***H$_2$***—C≡CH). The signals at 6.7 and 7.9 ppm are related to the protons on the benzene ring. The signal of the protons on the amino group (—N***H$_2$***) appears at 4.1 ppm. After a reaction with nitrosyl tetrafluoroborate, the diazonium salt of propargyl *p*-aminobenzoate was synthesized. FTIR spectra of propargyl *p*-aminobenzoate and its diazonium salt were shown in Supporting Information Figure S2. In FTIR spectrum of propargyl *p*-aminobenzoate, the absorption peaks at 3290 cm^{-1} and 2123 cm^{-1} are attributed to the stretching vibration of the unsaturated carbon–hydrogen bond of alkyne group and C≡C bond, respectively.[31] After reaction with nitrosyl tetrafluoroborate, the absorption peaks from —NH$_2$ groups at 3430 cm^{-1}, 3336 cm^{-1}, and 3213 cm^{-1} disappeared and a peak representing the N≡N stretching of

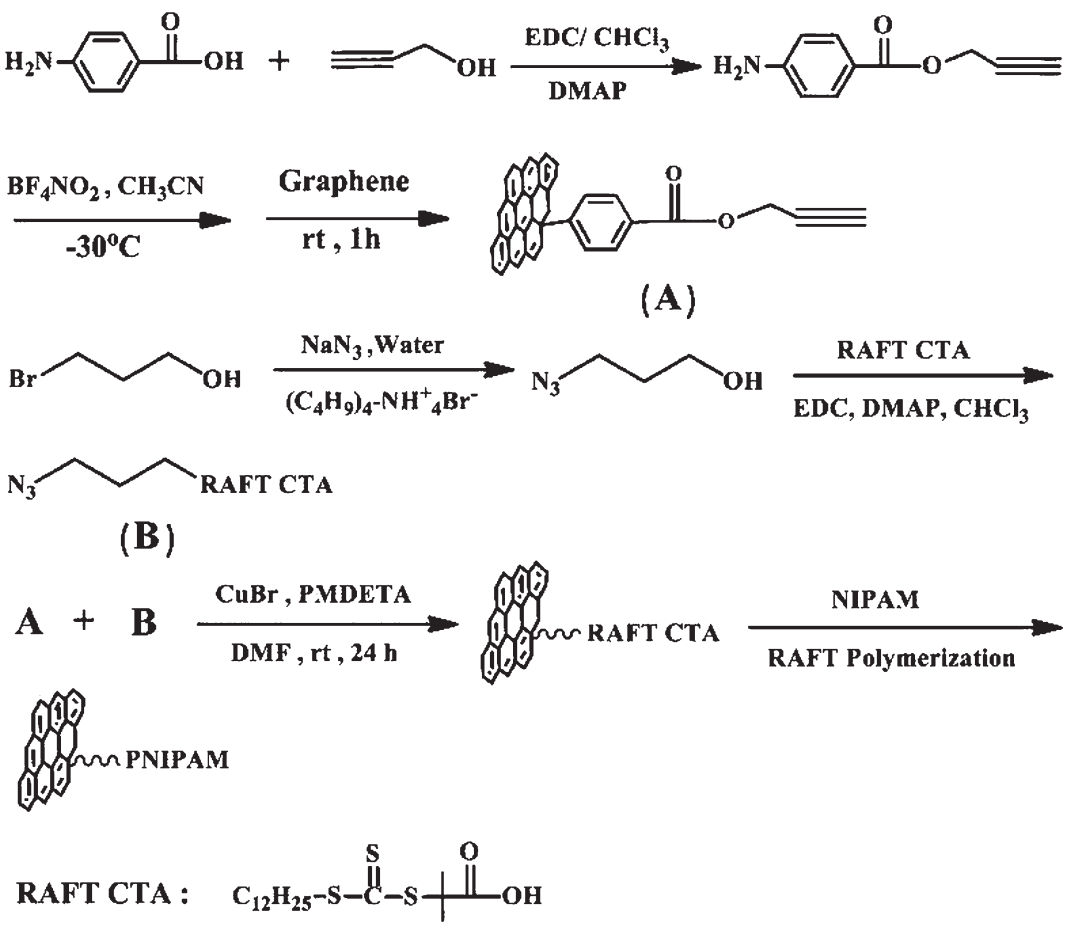

SCHEME 2 A scheme for the preparation of RAFT CTA-modified RGO, and *in situ* RAFT polymerization of NIPAM on the surfaces of RGO sheets.

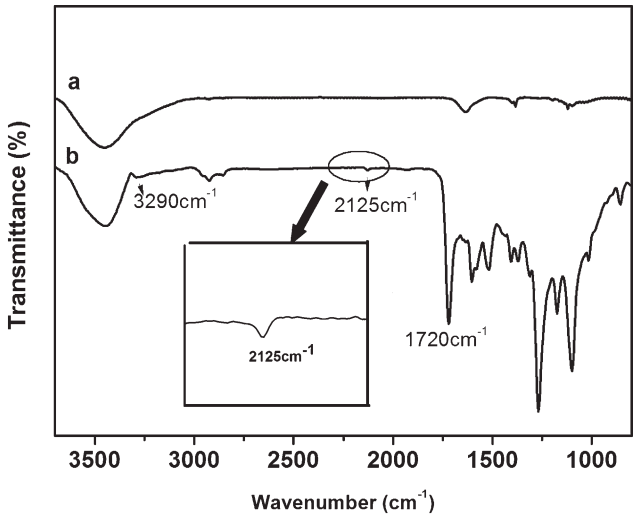

FIGURE 1 FTIR spectra of (a) RGO, (b) alkyne-functionalized RGO.

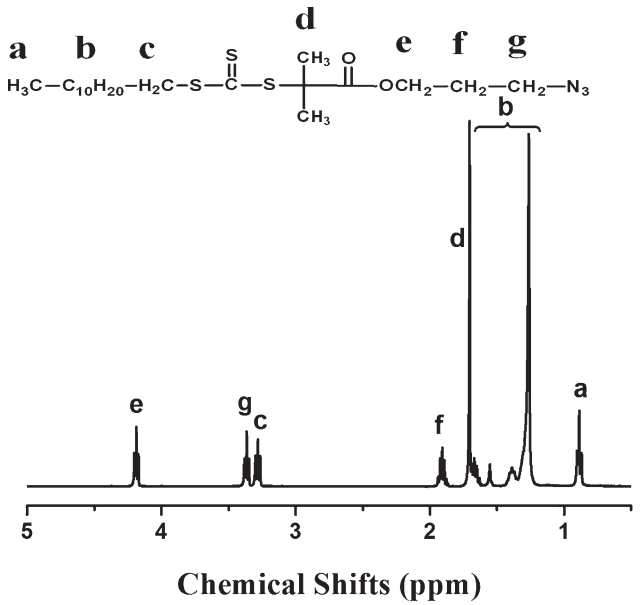

FIGURE 2 ^{1}H NMR spectrum of *S*-1-dodecyl-*S*′-(α,α′-dimethyl-α″-3-azido-1-propyl acetate) trithiocarbonate in $CDCl_3$.

the diazonium group appeared at 2,280 cm^{-1} (Supporting Information Fig. S2b), which confirmed the successful synthesis of diazonium salt.[6]

Alkyne-functionalized RGO was prepared by treatment of RGO dispersion with diazonium salt of propargyl *p*-aminobenzoate at room temperature overnight. FTIR spectra of RGO and alkyne-functionalized RGO are presented in Figure 1. After modification, the absorption peaks at 3290 cm^{-1} and 2,125 cm^{-1} representing the characteristic valence vibration of C≡CH, and the peak at 1,720 cm^{-1} from the C=O stretch were observed.[30]

S-1-Dodecyl-*S*′-(α,α′-dimethyl-α″-3-azido-1-propyl acetate) trithiocarbonate was synthesized by esterification of *S*-1-dodecyl-*S*′-(α,α′-dimethyl-α″-acetic acid) trithiocarbonate and 3-azido-1-propanol. ^{1}H NMR spectrum of the azido-terminated trithiocarbonate was shown in Figure 2. The peaks at 4.19 ppm [—COO—C***H₂***— $(CH_2)_2$—N_3] and 3.36 ppm (—C***H₂***—N_3) can be observed, which indicates the successful esterification of *S*-1-dodecyl-*S*′-(α,α′-dimethyl-α″-acetic acid) trithiocarbonate and 3-azido-1-propanol. On the spectrum the peaks from 1.27 ppm to 1.68 ppm are attributed to the 20 methylene proton [CH_3—(C***H₂***)***₁₀***—CH_2—], and the peak at 3.28 ppm (peak c) is related to the methylene protons [—C(S)S—C***H₂***—] next to the trithiocarbonate group. FTIR spectrum of azido-terminated trithiocarbonate is shown in Supporting Information Figure S3a. On the spectrum a strong absorption at 2,112 cm^{-1} representing the valence vibration of azide group, and an absorption peak at 1080 cm^{-1} representing the trithioester groups were observed.[32]

RAFT CTA-modified RGO was prepared by click reaction between azido-terminated trithiocarbonate and alkyne-functionalized RGO. FTIR spectra of azido-terminated trithiocarbonate and RAFT CTA-modified RGO are shown in Supporting Information Figure S3b. On the spectrum of RAFT CTA-modified RGO, an absorption peak at 1724 cm^{-1} representing the C=O stretch, and the characteristic peaks representing the trithioester groups at 1,072 cm^{-1} were observed.[30] Elemental analysis was used to determine the sulfur content and the amount of the RAFT CTA grafted to the RGO sheets. The elemental analysis result shows that the sulfur content is 3.27 wt %, so the RAFT CTA in the nanocomposite is about 0.34 mmol/g. XPS spectrum provides information on the type and number of different species of a given atom in the molecules. The RAFT CTA-modified RGO was also characterized by XPS. Figure 3 shows wide XPS spectra of unmodified and RAFT CTA-modified RGO. On the XPS spectrum of RAFT CTA-modified RGO, a peak at 162.5 eV corresponding to the binding energy of S_{2p} of the trithiocarbonate was observed. However, on the spectrum of RGO, no peak appeared at this position, which proved successful functionalization of RGO by RAFT CTA. PNIPAM on RGO sheets was prepared by *in situ* RAFT polymerization. Because of the

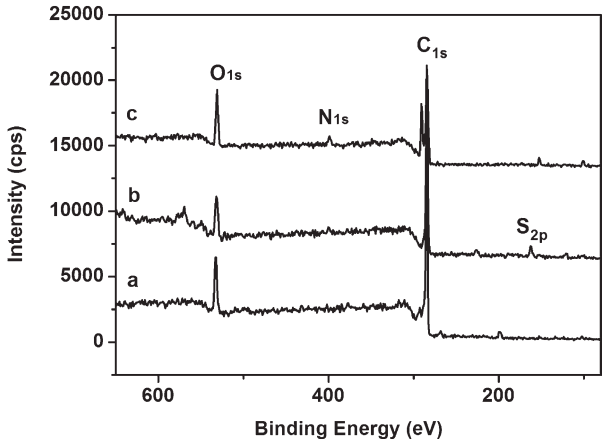

FIGURE 3 Wide XPS spectra of (a) RGO, (b) RAFT CTA-modified RGO, and (c) RGO with PNIPAM on the surfaces.

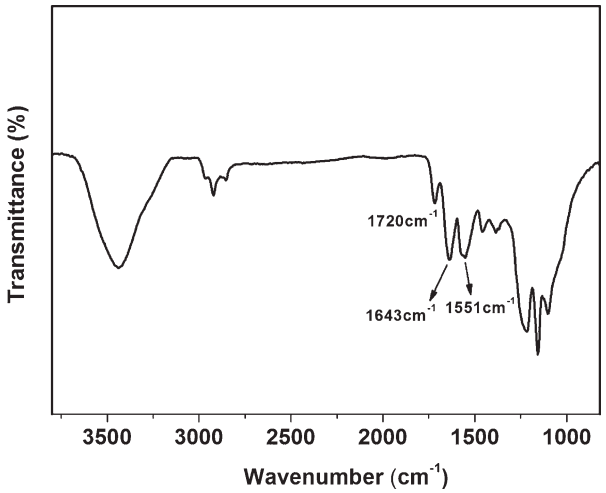

FIGURE 4 FTIR spectrum of PNIPAM on RGO sheets.

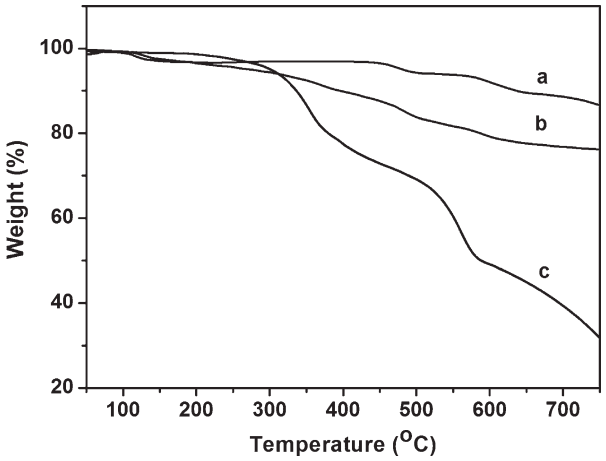

FIGURE 5 TGA curves of (a) RGO, (b) RAFT CTA-modified RGO, and (c) RGO sheets with PNIPAM on the surfaces.

difficulty in the direct measurement of the molecular weight of polymer chains prepared on the surfaces of RGO by living/controlled free radical polymerization, one way to determine the molecular weight of the grafted polymer chains was to add sacrificial initiator (or RAFT CTA) molecules into the polymerization system and measure the molecular weight of the free polymer produced in the solution, because it was reported that free polymers produced in the solution have almost the same molecular weight as those prepared on the solid substrates.[26,33,34] In this research, trace amount of free RAFT CTA was added to the reaction system, and the molecular weight of the free polymer produced in the solution was determined by GPC. The apparent molecular weight (M_n) and polydispersity index of PNIPAM were 19K and 1.77, respectively. ^{1}H NMR spectrum of the free PNIPAM in $CDCl_3$ was presented in Supporting Information Figure S4.

FTIR spectrum of RGO/PNIPAM nanocomposite is presented in Figure 4. A broad band at about 3500 cm^{-1} is attributed to the N—H stretching vibration of PNIPAM and the hydroxyl stretching vibration of the hydroxyl groups on RGO sheets. On the spectrum, the typical absorption peaks of PNIPAM include an absorption at 1643 cm^{-1} due to C=O stretching and an absorption at 1551 cm^{-1} from N—H stretching.[35]

RGO, RAFT CTA-modified RGO and RGO/PNIPAM nanocomposites were analyzed by TGA (Fig. 5). TGA of the original RGO was found to have 13 wt % weight loss in the range between 100 and 750 °C (curve a in Fig. 5), which was attributed to the loss of the functional groups such as COOH and OH groups on the sheets. Upon grafting of RAFT CTA, the composite was found to have 24 wt % weight loss (curve b in Fig. 5), and so approximately 11 wt % of the modified RGO was the RAFT CTA and the diazonium salt of propargyl *p*-aminobenzoate. After *in situ* RAFT polymerization, RGO/PNIPAM nanocomposite was found to have 68 wt % weight losses in the range between 280 °C and 750 °C (curve c in Fig. 5). Wide XPS spectrum of RGO/PNIPAM nanocomposites is presented in Figure 3. On the spectrum a peak at 399.9 eV corresponding to the N_{1s} binding energy of PNIPAM can be observed, which proves successful grafting of PNIPAM on RGO sheets. AFM is a direct method to observe the structure of the original RGO sheets. Figure 6 shows a tapping mode

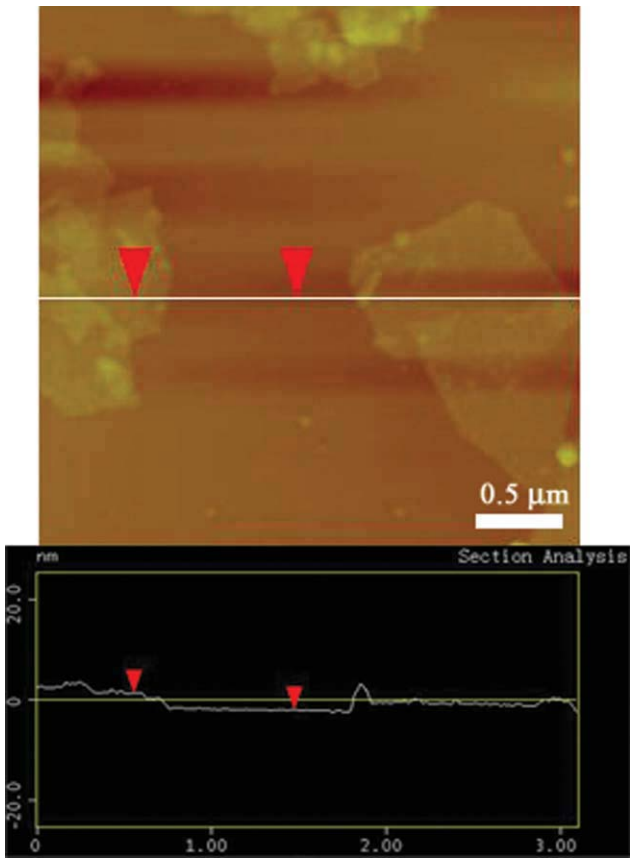

FIGURE 6 AFM image and height profile of RGO.

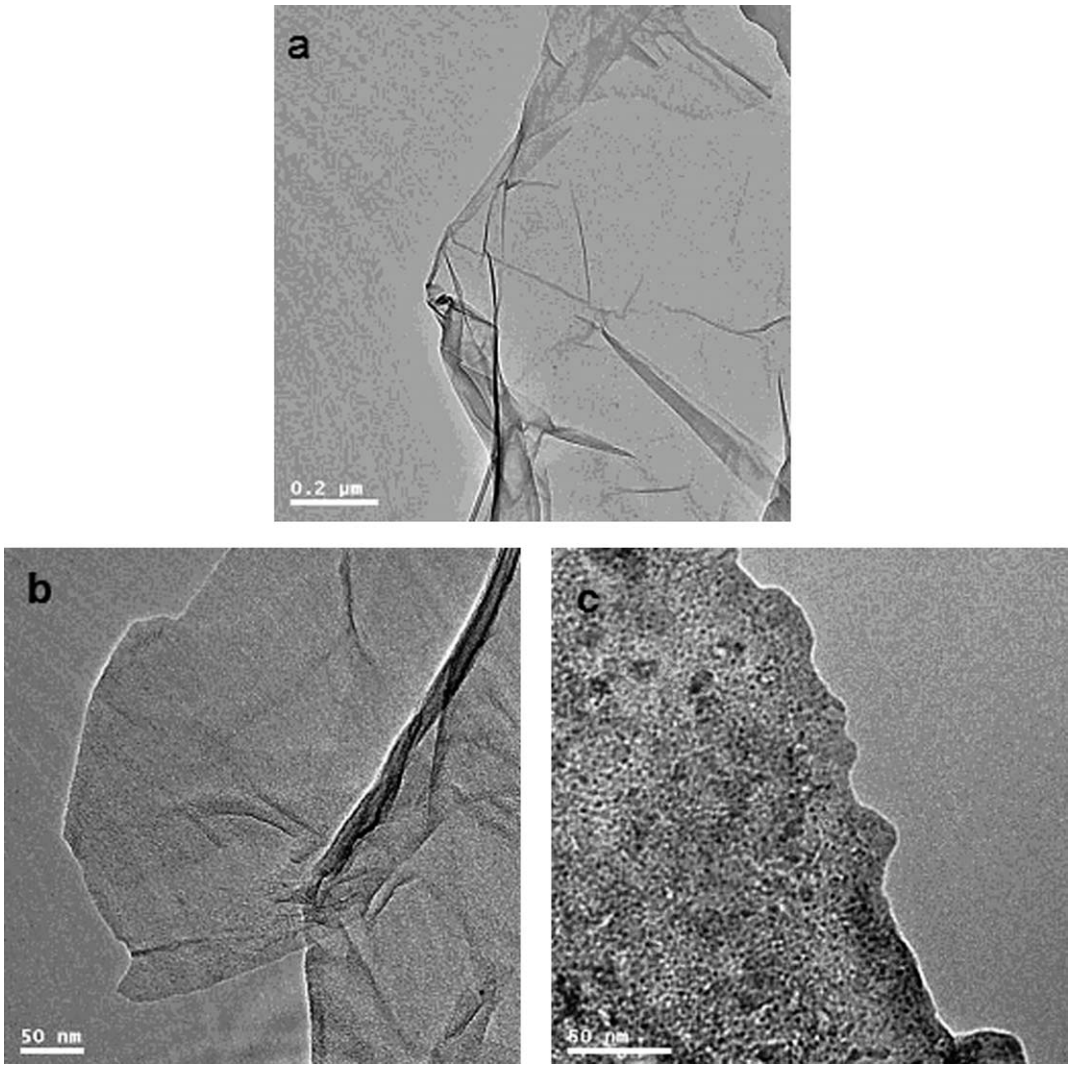

FIGURE 7 (a) A TEM image of RGO observed at low magnification; (b) a magnified TEM image showing the blank RGO surface; (c) a TEM image of RGO/PNIPAM nanocomposite. The dark dots on the surfaces of nanosheets represent PNIPAM domains.

AFM image of the original RGO sheets. The sample was prepared by depositing RGO aqueous dispersion (0.1 mg/mL) onto a new cleaved mica surface and dried under vacuum at room temperature. The cross-sectional view of the AFM image indicated that the height of the sheets ranged from 1.7 nm to 3 nm, or the flake of RGO had two or three layers.

The morphology of RGO and RGO/PNIPAM nanocomposite was studied by TEM. RGO or RGO/PNIPAM nanocomposite was dispersed in H_2O under sonication. TEM specimens were prepared by dipping copper grids into the solution and drying in air. Before TEM observation, the specimens were stained in OsO_4 atmosphere. Figure 7(a,b) are TEM images of RGO at different magnifications. On the two images blank RGO surfaces were observed. Figure 7(c) is a TEM image of RGO/PNIPAM nanocomposite. The dark dots on the surface of RGO sheet represent PNIPAM nanosized domains. In aqueous solution, the grafted PNIPAM chains are extended due to the solubility of the polymer chains in water; however, after

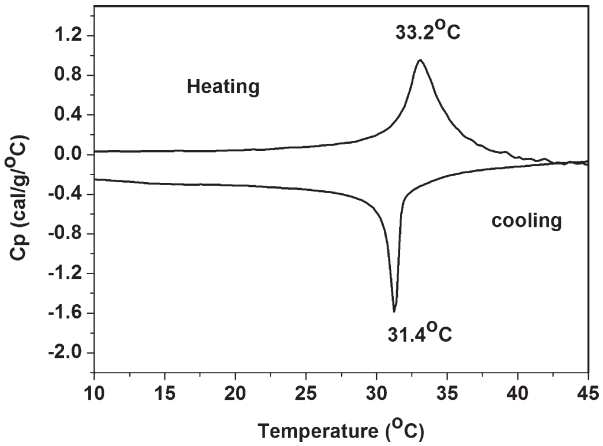

FIGURE 8 Microcalorimetric endotherm recorded for aqueous dispersion of RGO/PNIPAM nanocomposites. In the measurements, the heating rate and cooling rate were both set at 1 °C/min, and the nanocomposites concentration was 2 g/L.

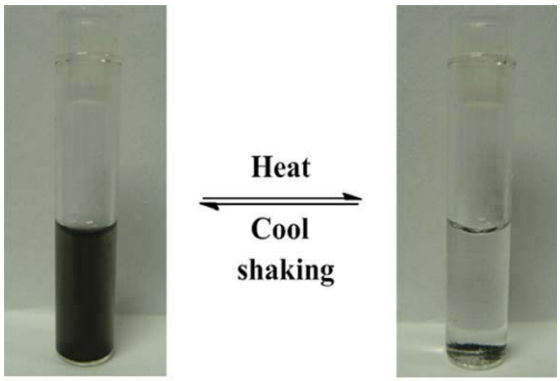

FIGURE 9 Thermal turbidity testing of RGO/PNIPAM composite in H_2O.

drying PNIPAM chains collapse onto the surfaces of RGO sheets forming nanosized domains. The average size of PNIPAM domains is about 2 to 3 nm.

PNIPAM is a thermosensitive polymer, which undergoes phase transition at its lower critical solution temperature (LCST) because of the cooperative dehydration of PNIPAM chains and concomitant collapse of individual chains from hydrated coils to hydrophobic globules.[36,37] To determine the LCST of PNIPAM on RGO surface, micro-DSC measurement of the aqueous dispersion of RGO/PNIPAM was performed. Figure 8 shows the temperature dependence of the specific heat capacity (C_p) in one heating and cooling cycle. The result shows that PNIPAM on RGO has a LCST transition at 33.2 °C in the heating process and at 31.4 °C in the cooling process. The difference of the two values should be attributed to some additional intrachain hydrogen bondings among PNIPAM chains formed in the collapse state at high temperatures.[38,39] The thermosensitivity of RGO/PNIPAM composites was also monitored by using turbidity measurements. When the temperature of RGO/PNIPAM dispersion was above the LCST of PNIPAM, the graphene/PNIPAM suspension precipitated at the bottom of the vial, and the RGO/PNIPAM aggregates could be redispersed rapidly by cooling down below the LCST (Fig. 9).

CONCLUSIONS

Azide-terminated RAFT CTA was synthesized and introduced to the surfaces of RGO by click reaction. PNIPAM brushes on the RGO sheets were successfully prepared by RAFT polymerization. The research reported in this manuscript proves that combination of click chemistry and RAFT polymerization is a general and powerful tool in the preparation of RGO/polymer nanocomposites. More researches on the synthesis of new functional RGO/polymer nanocomposites based on this method are being under investigation at this time.

This project was supported by National Natural Science Foundation of China under contract no. 20904009 and the Science and Technology Committee of Tianjin under contract no. 10JCYBJC01900TD.

REFERENCES

1 Geim, A. K.; Novoselov, K. S. *Nat Mater* **2007,** *6*, 183–191.

2 Novoselov, K. S.; Geim, A. K.; Morozov, S. V.; Jiang, D.; Zhang, Y.; Dubonos, S. V.; Grigorieva, I. V.; Firsov, A. A. *Science* **2004,** *306*, 666–669.

3 Wu, J.; Pisula, W.; Mullen, K. *Chem Rev* **2007,** *107*, 718–747.

4 Zhang, Y.; Tan, Y. W.; Stormer, H. L.; Kim, P. *Nature* **2005,** *438*, 201–204.

5 Freitag, M.; Steiner, M.; Martin, Y.; Perebeinos, V.; Chen, Z.; Tsang, J. C.; Avouris, P. *Nano Lett* **2009,** *9*, 1883–1888.

6 Lomeda, J.; Doyle, C.; Kosynkin, D.; Hwang, W.; Tour, J. *J Am Chem Soc* **2008,** *130*, 16201–16206.

7 Xu, Y. X.; Bai, H.; Lu, G. W.; Li, C.; Shi, G. Q. *J Am Chem Soc* **2008,** *130*, 5856–5857.

8 Liu, J.; Yang, W.; Tao, L.; Li, D.; Boyer, C.; Davis, T. P. *J Polym Sci Part A: Polym Chem* **2010,** *48*, 425–433.

9 Mackie, I. D.; DiLabio, G. A. *J Phys Chem A* **2008,** *112*, 10968–10976.

10 Lee, S. H.; Dreyer, D. R.; An, J.; Velamakanni, A.; Piner, R. D.; Park, S.; Zhu, Y.; Kim, S. O.; Bielawski, C. W.; Ruoff, R. S. *Macromol Rapid Commun* **2010,** *31*, 281–288.

11 Shen, J.; Hu, Y.; Li, C.; Qin, C.; Ye, M. *Small* **2009,** *5*, 82–85.

12 Zhang, B.; Yu, B.; Kang, E.-T.; Zhu, J.; Li, Y. *J Polym Sci Part A: Polym Chem* **2010,** *48*, 2642–2649.

13 Zhuang, X.; Chen, Y.; Liu, G.; Li, P. P.; Zhu, C.; Kang, E. T.; Neoh, K. G.; Zhang, B.; Zhu, J. H.; Li, Y. *Adv Mater* **2010,** *22*, 1731–1735.

14 Liu, L. H.; Yan, M. D. *Nano Lett* **2009,** *9*, 3375–3378.

15 Sharma, R.; Baik, J. H.; Perera, C. J.; Strano, M. S. *Nano Lett* **2010,** *10*, 398–405.

16 Quintana, M.; Spyrou, K.; Grzelczak, M.; Browne, W. R.; Rudolf, P.; Prato, M. *ACS Nano* **2010,** *4*, 3527–3533.

17 Kolb, H. C.; Finn, M. G.; Sharpless, K. B. *Angew Chem Int Ed Engl* **2001,** *40*, 2004–2021.

18 Sun, S.; Cao, Y.; Feng, J.; Wu, P. *J Mater Chem* **2010,** *20*, 5605–5607.

19 He, H.; Gao, C. *Chem Mater* **2010,** *22*, 5054–5064.

20 Harvison, M. A.; Lowe, A. B. *Macromol Rapid Commun* **2011,** *32*, 779–800.

21 Li, Y.; Benicewicz, B. C. *Macromolecules* **2008,** *41*, 7986–7992.

22 Fu, G. D.; Xu, L. Q.; Yao, F.; Zhang, K.; Wang, X. F.; Zhu, M. F.; Nie, S. Z. *ACS Appl Mater Interface* **2009,** *1*, 239–243.

23 Zhang, X.; Lian, X.; Liu, L.; Zhang, J.; Zhao, H. *Macromolecules* **2008,** *41*, 7863–7869.

24 Zhao, C.; Wu, D.; Lian, X.; Zhang, Y.; Song, X.; Zhao, H. *J Phy Chem B* **2010,** *114*, 6300–6308.

25 Lian, X.; Jin, J.; Tian, J.; Zhao, H. *ACS Appl Mater Interface* **2010,** *2*, 2261–2268.

26 Yang, Y.; Wang, J.; Zhang, J.; Liu, J.; Yang, X.; Zhao, H. *Langmuir* **2009,** *25*, 11808–11814.

27 Lai, J. T.; Filla, D.; Shea, R. *Macromolecules* **2002,** *35*, 6754–6756.

28 Staudenmaier, L. *Ber Dtsch Chem Ges* **1898,** *31*, 1481–1487.

29 Schniepp, H. C.; Li, J. L.; McAllister, M. J.; Sai, H.; Herrera-Alonso, M.; Adamson, D. H.; Prud'homme, R. K.; Car, R.; Saville, D. A.; Aksay, I. A. *J Phys Chem B* **2006,** *110*, 8535–8539.

30 Boyer, C.; Liu, J. Q.; Bulmus, V.; Davis, T. P.; Barner-Kowollik, C.; Stenzel, M. H. *Macromolecules* **2008,** *41*, 5641–5650.

31 Jin, Z.; Lomeda, J. R.; Price, B. K.; Lu, W.; Zhu, Y.; Tour, J. M. *Chem Mater* **2009,** *21*, 3045–3047.

32 Lian, X.; Wu, D.; Song, X.; Zhao, H. *Macromolecules* **2010,** *43*, 7434–7445.

33 Rowe, M. D.; Hammer, B. A. G.; Boyes, S. G. *Macromolecules* **2008,** *41*, 4147–4157.

34 Grande, C. D.; Tria, M. C.; Jiang, G.; Ponnapati, R.; Advincula, R. *Macromolecules* **2011,** *44*, 966–975.

35 Liu, Y. X.; Tu, W. X.; Cao, D. P. *Ind Eng Chem Res* **2010,** *49*, 2707–2715.

36 Heskins, M.; Guillet, J. E. J. *Macromol Sci* **1968,** *2*, 1441–1455.

37 Schild, H. G. *Prog Polym Sci* **1992,** *17*, 163–249.

38 Ding, Y.; Ye, X.; Zhang, G. *Macromolecules* **2005,** *38*, 4403–4408.

39 Wu, C.; Wang, X. *Phys Rev Lett* **1998,** *80*, 4092–4094.